Response of stone wool-insulated building barriers under severe heating exposures

Original Manuscript

Corresponding Author:
Blanca Andres,
Danish Institute of Fire and Security Technology, Jernholmen 12, Hvidovre DK-2650, Denmark
Email: bav@dbigroup.dk

Response of Stone Wool Insulated Building Barriers under Severe Heating Exposures

Blanca Andres[1,2], Karlis Livkiss[1,2], Juan.P. Hidalgo[3], Patrick van Hees[2], Luke Bisby[4], Nils Johansson[2], Abhishek Bhargava[1,2]

[1] Danish Institute of Fire and Security Technology, Hvidovre DK-2650, Denmark

[2] Division of Fire Safety Engineering, Lund University, Lund SE-22100, Sweden

[3] School of Civil Engineering, The University of Queensland, Brisbane, St. Lucia, QLD 4072, Australia

[4] School of Engineering, The University of Edinburgh, Edinburgh EH9 3JL, UK

Abstract

This paper presents the experimental results of stone wool layered sandwich constructions, with either steel or gypsum claddings, tested under four different heating exposures: a 7 kW/m^2 incident radiant heat flux exposure, a 60 kW/m^2 incident radiant heat flux exposure, a parametric time-temperature curve exposure, and the ISO 834 standard time-temperature exposure. The test apparatus used were: a movable radiant panel system, a mid-scale furnace (1.5 m^3), and a large-scale furnace (15 m^3). The results show that reduced-scale tests are capable of reproducing the heat transferred through the construction at large scale provided there is limited mechanical degradation. The results indicate that the availability of oxygen is fundamental to the fire behaviour of the sandwich composites tested. Reactions occurring in stone wool micro-scale testing, such as oxidative combustion of the binder or crystallization of the fibres, have a limited effect on the temperature increase when wool is protected from air entrainment.

Keywords

Stone Wool Insulated Sandwich Panels, Building Fire Barriers, Full Scale Experiments, Intermediate Scale Experiments, Severe Heat Exposures, Furnace Test, H-TRIS Test

Introduction

The adequate fire response of a building requires provision of sufficient egress time to evacuate the building and undertake fire-fighting operations before its structural capacity is significantly affected. Building fire barriers are compartmentation elements within a building that limit the spread of fire to neighbouring compartments. Thus, they are used to ensure adequate safety levels and play a major role in the overall fire safety strategy for the building. Building fire barriers are, in many cases, layered composite constructions composed of panels attached to timber or cold-formed stud systems. The interior of the constructions can be left empty as a cavity construction, or in some cases can be filled in with insulation material to achieve better thermal and acoustic performance. Common insulation materials are mineral wools (i.e. stone or glass wool) or plastics (rigid polyisocyanurate, polyurethane, phenolic foams, or expanded polystyrene). Facing panels provide both in plane and out of plane strength and stiffness, and stability to the construction and comprise steel plates, gypsum plasterboards, timber chipboards, etc.

Building fire barriers are traditionally assessed and certified based on standard fire-resistance tests (1). However, a global trend moving towards explicit performance-based design approaches means that there is a growing interest in developing predictive models for the behaviour of constructions in different (i.e. non-standardised) design fire scenarios; including similar situations to the ones the building is likely to experience in a real fire event. Models also used in many cases to provide performance based assessment on non-rated constructions under standard fire tests. Numerous modelling attempts are presented in the literature to predict the response of building elements under standard heating exposures (2–7). A common approach has been to build models by fitting input empirical material properties that simplify the complex thermo-physical phenomena (mass transfer, pyrolysis, etc.) to standard furnace test results (3,8,9). However, in most cases, these models fail to predict response under design fire exposures other than the ones against which they have been validated/fitted (10). The development of models capable of predicting fire behaviour, especially in non-standard or non-furnace scenarios, requires a deep understanding of the influencing phenomena, thus necessitating scenario-independent predictive models. Systematic experimental analyses that characterise phenomena under different heating exposures, with adequate instrumentation, can provide material properties capable of being used to model different fire scenarios (11). Studies in the literature that compare the response of the same constructions under different heat exposures are limited, in many cases, comparing standard furnace exposures to natural fires (4,5,12) without looking in detail into the nature of the phenomena occurring.

This study presents the experimental results of stone wool layered sandwich constructions, with either steel or gypsum claddings, tested under four different heating exposures. The experimental programme aims to identify phenomena occurring in each of the materials affecting the heat transfer, along with the interactions between them in a systematic way that would help developing scenario-independent models. The method followed consists of a "*multi-scale*" approach, where the materials are investigated at smaller scale under different heating exposures; the knowledge obtained is used to predict the behaviour at larger scales (Figure 1). The paper presents experimental results from mid-scale and full-scale tests on stone wool layered composites. Previous research has focused on micro-scale (few milligram samples) and solid material scales (<500 cm^2)(13,14). This work serves as basis for modelling the behaviour of the constructions; the modelling outcomes are presented elsewhere.

Methodology

Figure 1 shows the scales involved in the multi-scale approach implemented herein. In particular, the current paper focuses on experimental results from composite mid-scale and full-scale testing, shown in Figure 1 as Phase I-IV. Prior micro-scale analysis of the behaviour of stone wool in thermogravimetric analysis (TGA) and micro-combustion calorimetry (MCC) (13–17) has shown two mass loss reactions occurring in the wool in air, followed by a gain in mass. The first reaction occurs between 200 and 400 °C, the second one between 400 and 600 °C, and the third one above 700 °C. The first two reactions correspond to the pyrolysis and oxidation of the organic binder content in the wool, respectively, and the third is associated with the crystallization of the fibres. In a nitrogen atmosphere, a single reaction is observed between 200 and 400 °C corresponding to the pyrolysis of the organic binder content. The value of mass lost during those reactions is different depending on the wool, but was less than 6 % in air, and 3 % in nitrogen for the materials tested herein. Tests with a slug calorimeter (18,19), used to determine the thermal conductivity of the stone wool at higher temperatures characteristic of a fire, have shown exothermic reactions occurring in the wool at around 200 to 450 °C and 800 to 900 °C (14,20) when heated at a constant rate.

In Phase I, Steel-Stone wool sandwich (S-SW-S) composites were tested under: (1) a low level of irradiation (7 kW/m²), and (2) a high level of irradiation (60 kW/m²). Based on heat transfer calculations, only the first reaction described above was expected to occur in a small part of the wool thickness at 7 kW/m², whereas at 60 kW/m² all the reactions should occur. In Phase II, Gypsum-Stone wool sandwich (G-SW-G) specimens were tested under the same constant incident radiant heat fluxes to identify other phenomena such as burning of the paper lining of the gypsum plasterboards, water transport along the building assembly, and cracking of the board which could increase heat transfer to the insulation. While phases I and II investigated composite behaviour under a constant incident radiant heat, Phase III investigated the same constructions under variable heat flux exposures. The main goal of Phase III was to identify whether the phenomena occurring at constant heat exposures were also present under variable heat exposures, which represent common scenarios that full-scale specimens are exposed to. During Phase IV, a full-scale G-SW-G wall was tested in an attempt to link the behaviour between intermediate and full scales, and to detect other phenomena affecting the overall performance, e.g. thermal bowing or cracking.

		Objective	Test conditions
	**Micro-scale** Thermogravimetrical analysis, MCC, Bomb calorimetry	Reactions occurring in the wool	5, 10, 20 K/min Air and Nitrogen atmospheres
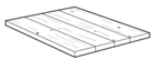	**Material-scale** Modified Slug-Calorimetry	Thermal properties of wool	5, 15 K/min
	Phase I-Composite Steel-Stone wool sandwich (S-SW-S)	Behaviour of the wool in a composite	Low incident heat flux (7 kW/m²) High incident heat flux (60 kW/m²)
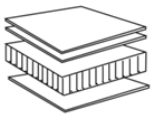	**Phase II-Composite** Gypsum-Stone wool sandwich (G-SW-G)	Other phenomena such as: burning of paper, moisture movent and condensation from gyspum	Low incident heat flux (7 kW/m²) High incident heat flux (60 kW/m²)
	Phase III-Composite S-SW-S & G-SW-G	Presence of the identified phenomena in variable complex incident heat fluxes	Standard ISO 834 Variable incident heat flux
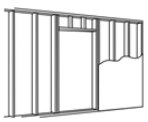	**Phase IV-Full Scale** G-SW-G	Full scale system behaviour , effect of joints, thermal bowing, cracking of boards	Standard ISO 834

Figure 1: Multi-scale Experimental Methodology

Experimental work

Materials

The two types of layered constructions (S-SW-S & G-SW-G) selected for this analysis represent a wide range of applications for building barriers, such as commercial or industrial for S-SW-S and residential for G-SW-G. The choice of constructions was made due their widespread use in buildings as compartmentation elements. A detailed description of the composites tested can be found in Tables 1 and 2.

Table 1: List of Experiments Performed

Test Id.	Construction	Test Apparatus	Exposures	Number of repeated tests	Cross-section	Dimensions	Exposed area
A	S-SW3-S	H-TRIS	Low constant incident radiant heat flux	2	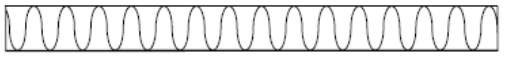	0.7 mm steel 45 mm stone wool	500 x 500 mm²
B	S-SW3-S	H-TRIS	High constant incident radiant heat flux	2		0.7 mm steel 45 mm stone wool	500 x 500 mm²
C	G2-SW1-G2	H-TRIS	Low constant incident radiant heat flux	2	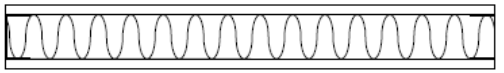	9.5 mm gypsum 45 mm stone wool 45 mm steel stud	500 x 500 mm²
D	G2-SW1-G2	H-TRIS	High constant incident radiant heat flux	2	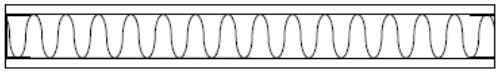	9.5 mm gypsum 45 mm stone wool 45 mm steel stud	500 x 500 mm²
E	S-SW3-S	H-TRIS	Parametric like incident radiant heat flux	2		0.7 mm steel 45 mm stone wool	500 x 500 mm²
F	G2-SW1-G2	H-TRIS	Parametric like incident radiant heat flux	2	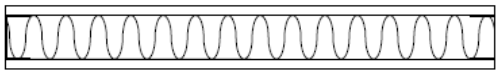	9.5 mm gypsum 45 mm stone wool 45 mm steel stud	500 x 500 mm²
G	S-SW3-S	Mid-Scale Furnace	Standard ISO 834	2	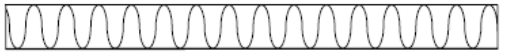	0.7 mm steel 45 mm stone wool	500 x 500 mm²

Test Id.	Construction	Test Apparatus	Exposures	Number of repeated tests	Cross-section	Dimensions	Exposed area
H	S-SW4-S	Mid-Scale Furnace	Standard ISO 834	2	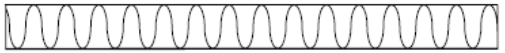	0.7 mm steel 45 mm stone wool	500 x 500 mm²
I	G1-SW1-G1	Mid-Scale Furnace	Standard ISO 834	2	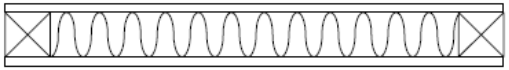	9.5 mm gypsum 45 mm stone wool 45 mm wood stud	500 x 500 mm²
J	G1-SW2-G1	Mid-Scale Furnace	Standard ISO 834	2	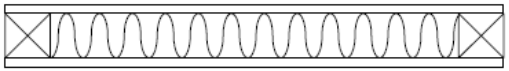	9.5 mm gypsum 45 mm stone wool 45 mm wood stud	500 x 500 mm²
K	G1-SW1-G1	Large Furnace	Standard ISO 834	1	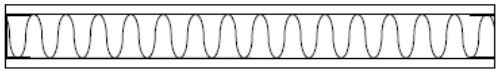	9.5 mm gypsum 45 mm stone wool 45 mm steel stud	3000x3000 mm²

Table 2: Ambient temperature materials properties for the materials used in this study

Material	Density (kg/m^3)	Thermal Conductivity (W/m·K)	Water Content (%)	Organic Binder (%)
Gypsum 1	650	0.19	18.4	-
Gypsum 2	850	0.25	18.0	-
SW1	36.8	0.037	-	2.5 ± 0.06
SW2	60.7	0.033	-	3.75 ± 0.01
SW3	85.0	0.041	-	-
SW4	153.6	0.04	-	3.48 ± 0.07
Stainless Steel	7805	15	-	-

Stainless steel is a highly conductive material with an ambient thermal conductivity of 15 W/m·K rising to 30 W/m·K at 1200 °C (21). In common fire scenarios, with convective heat transfer coefficient (hc) varying between 4-60 $W/m^2 \cdot K$ (22), and steel thickness smaller than 25 mm the Biot number ($\frac{h_c \cdot L}{k}$) is sufficiently small (< 0.1) to assume that there is no thermal gradient through the cross-section. This provides valuable information about the heat exposure to the wool in contact with the steel plate, limited to the contact in between the stone wool and the steel plate. The properties of steel are shown in Table 2 from the literature (21). Stone wool is a permeable insulation material, composed of rock fibres and a small percentage of organic binder that hold the fibres together, and a smaller amount of oil that makes the product water repellent (23,24). Although according to its Euroclass (25) it is class A1 or A2, stone wool is a non-combustible material, the small percentage of organic binder that it contains undergoes an exothermic reaction during heating in air, potentially increasing the temperature inside the insulation (15,20,26). Four different types of stone wool were used in the current study (SW1-4); SW1 and SW2 are lower density wools used in gypsum constructions, and SW3 and SW4 are higher density wools used in steel assemblies. Their densities, organic content, and ambient thermal conductivity are shown in Table 2. The density was measured on 4 to 6 samples giving a deviation of ± 2.5 kg/m^3. The organic content was measured by heating samples at 500 °C for one hour and measuring the mass loss. The value of ambient temperature thermal conductivity of the stone wool was given by the manufacturer. Gypsum plasterboards are composed of dehydrated calcium sulphate. Gypsum dehydrates when heated following a two-step endothermic reaction scheme (8). During the first reaction, calcium sulphate dehydrates to a hemihydrate form releasing 75 % of its water content; the remaining water is released in the second reaction. The first reaction occurs between 100 and 150 °C, and the second above 200 °C depending on the heating conditions (27,28). The endothermic nature of the reactions delays the transfer of heat

through the neighbouring materials when used in composites, this being a fundamental reason for its extensive use in buildings. The density of the gypsum plasterboards was measured prior to the test and includes the paper lining. The water content of gypsum plasterboards was obtained by heating up samples to 150 °C until the weight loss was constant; therefore, the value of water content in Table 2 includes free and chemically bound water.

Heat Exposures

The four different heating schemes mentioned in Table 1 and Figure 1 were: (1) a low constant incident radiant heat flux of 7 kW/m²; (2) a high constant incident radiant heat flux of 60 kW/m²; (3) a standard ISO 834 time-temperature curve; and (4) parametric-like incident radiant heat exposure. The parametric-like incident radiant heat exposure is a heat exposure used to reproduce the conditions in a defined compartment fire defined as room temperature. A more detailed description is provided below.As opposed to micro- and solid-scale testing, samples were heated only from one side, so heat is being transferred to a cold surface as would be in furnace testing or real fire conditions. The standard ISO 834 heating exposure was performed in a mid-scale furnace and a full-scale furnace. The parametric-like incident heat flux was performed at intermediate scale with a radiant panel (H-TRIS (29)). The procedure to determine the target heat flux for the H-TRIS testing was:

1. A hypothetical compartment of 20 m^2 was considered to represent a common scenario of characteristics: 20 m² floor area, 32 MJ/m² fire load, and standard openings of windows and doors (equivalent to an opening factor of 0.04 $m^{1/2}$) and plasterboard boundaries.
2. Using these values, the temperature-time exposure of the gas in the hypothetical compartment was calculated using the Swedish Method (30).
3. This temperature-time curves are translated to net heat flux to the surface of the hypothetical compartment. For this, convection and radiation boundary conditions are used and heat transfer calculations through the wall are performed, assuming a convective heat transfer coefficient of 25 W/K·m^2 and an emissivity of 0.9.

$$\boldsymbol{\varepsilon \cdot \sigma \cdot \left(T_{room}{}^{4} - T^{4}\right) + h_c \cdot \left(T_{room} - T\right) = -k \cdot \frac{\delta T}{\delta x}} \qquad [1]$$

   where ε is the emissivity of the material, σ is the Stefan-Boltzmann constant, T is the temperature of the exposed panel, T_{room} is the calculated hypothetical compartment temperature, and h_c is the convective heat transfer coefficient, and k is the thermal conductivity of the material
4. The net heat flux was then set as the testing target in H-TRIS.

The four different exposures are shown in Figure 2 as the unexposed temperature measurements of the exposed steel panel on S-SW-S composites. The lines represent the mean value measured, and the shaded areas the standard deviation. The temperature of the exposed steel panel at 7 kW/m³ remained below 300 °C, whereas on the three other heating exposures reached 700 °C. The parametric-like incident radiant heat exposures peaked at around 10 minutes to 750 °C, and was followed by a cooling phase. At 60 kW/m³, the temperature rose faster and then was maintained constant at around 750 °C.

In the standard ISO 834 exposure, there was a lower temperature demand at initial times, however, the temperature kept increasing up to 850 °C.

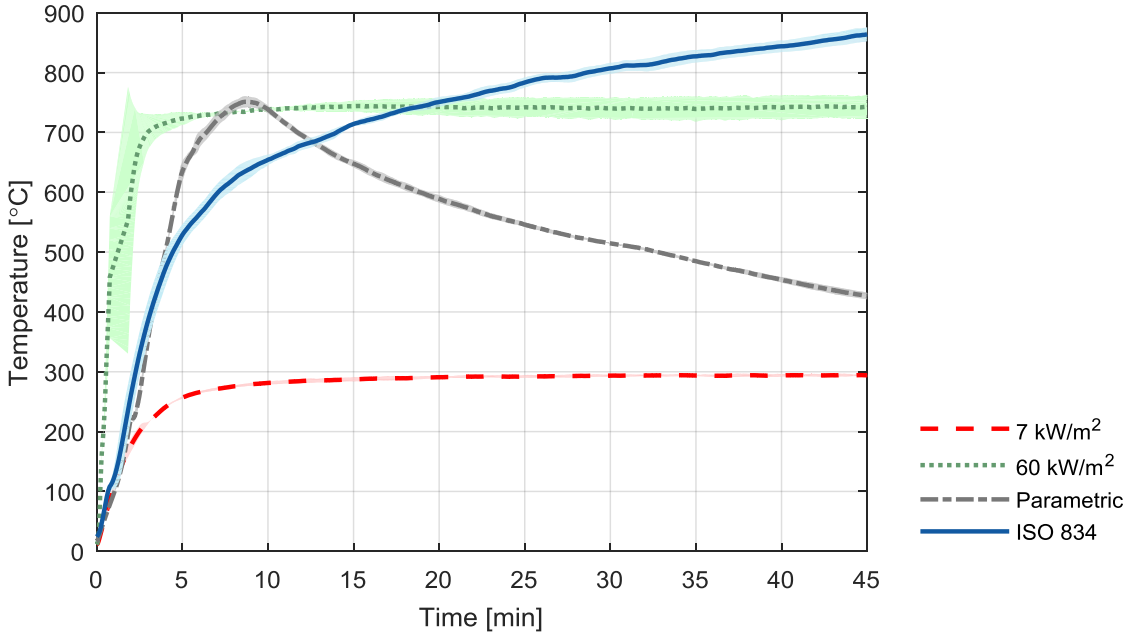

Figure 2: Heat exposure as temperature on the unexposed side of the exposed steel panel

Testing Apparatus

H-TRIS

The Heat-Transfer Rate Inducing System (29) (H-TRIS) is a novel fire testing methodology that consists of four propane-fired radiant panels placed on a linear motion system (Figure 3). The incident radiative heat flux to which the specimen is subjected is calibrated with regards to the distance to the radiant panels. Therefore, almost any time-history incident radiative heat exposure can be achieved; limited only by the minimum distance to the tested specimen and the type and size of the radiant panels. The heat delivered in H-TRIS considering the losses due to radiation and convection of the specimen to the surroundings, following the formulation in Equation 2.

$$\boldsymbol{\alpha \cdot \dot{q}''_{in} = \dot{q}''_{net} + \varepsilon \cdot \sigma \cdot T^4 + h_c \cdot (T - T_{amb})} \qquad [2]$$

where α is the absorptivity of the specimen, $\dot{q}''_{in}$ is the effective/lumped incident radiant heat flux at the surface of the specimen, $\dot{q}''_{net}$ is the net heat flux to the specimen, ε is the emissivity of the material, σ is the Stefan-Boltzmann constant, T is the temperature of the exposed panel, T_{amb} is the ambient temperature, and h_c is the convective heat transfer coefficient. The radiant panel is set as $\boldsymbol{\alpha \cdot \dot{q}''_{in}}$ so the net flux to the surface is $\boldsymbol{\dot{q}''_{net}}$. The convective heat transfer coefficient can be calculated using empirical correlations for external free convection flows in vertical plates (31) based on the Nusselt number and the characteristic length.

H-TRIS can be used as an extrapolation tool for full-scale fire tests, limited to a 1-D heat transfer through composite panels. The H-TRIS methodology was used to expose

the 500 mm² surface area specimens to constant and variable incident radiant heat exposures: (1) 7 kW/m²; (2) 60 kW/m²; and (3) variable incident heat flux (simulated parametric fire curve) (Table 1).

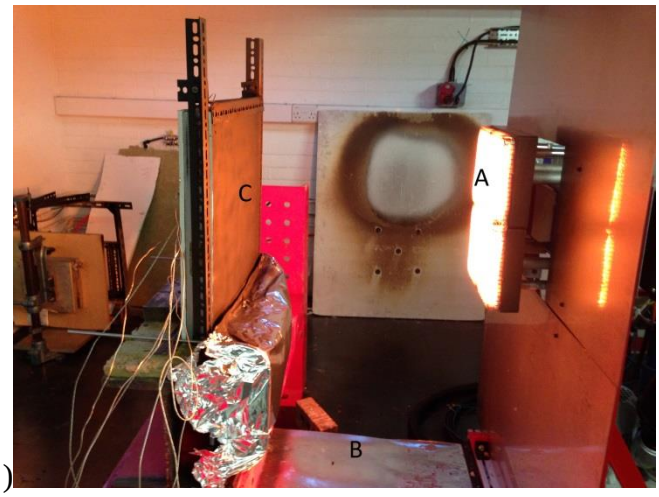

)

Figure 3: The Heat Transfer Rate Inducing System (H-TRIS): (A) Radiant Panels, (B) Specimen Tested (C) Motion System.

Mid- Scale Furnace

The mid-scale furnace has inner dimensions of 1.46 x 1.46 x 1.5 m^3. The furnace is shown in Figure 4. Four gas burners located on the walls supply energy by combustion of propane gas. The temperature inside the furnace is controlled by four plate-thermocouples as specified in EN 1363-1. The pressure is regulated by adjusting the exhaust of air, and it is kept around 20 Pa pressure difference. The walls of the furnace are made of ceramic fibre (200 kg/m^3) and the floor is made of bricks (850 kg/m^3). A 100 mm thick concrete frame with four holes, allows testing four specimens of 500 mm^2, simultaneously. The frame is placed on top of the furnace, thus the specimens are placed vertically. During the test, the samples are exposed to a standard ISO 834 on one of their sides and ambient lab conditions on the other side. Samples tested in the mid-scale furnace have the same exposed area as in H-TRIS. The readings from a thermocouple placed close to the edge compared to thermocouples placed in the middle specimen showed no tangible difference, thus the system reproduces a one-dimensional heat transfer.

Figure 4: Mid-scale furnace

Large Furnace

The large-scale test was performed in a vertical furnace at *The Danish Institute of Fire and Security Technology* in accordance with EN 1363 (32). The internal dimensions of the furnace are 3.2 x 3.2 x 1.5 m^3. The inside of the furnace is lined with two layers of fire bricks. The furnace has twelve propane gas burners located on the walls. Each burner has a power of 210 kW. The temperature inside the furnace is controlled by sixteen plate thermocouples following the ISO 834 standard fire curve, and a maximum pressure difference at the top of the furnace of 20 Pa.

Experimental Results

Constant incident heat fluxes intermediate scale (Phase I & II)

Figures 6 and 7 show the temperature measurements for tests A-D (Table 1), Figure 6(a) and 7(a) correspond to S-SW3-S constructions and Figure 6(b) and 7(b) correspond to G2-SW1-G2. Temperatures were measured on the unexposed side of the exposed panels (Exp) and on the unexposed side of the unexposed panel (Unexp) with type K thermocouples welded to a copper disk attached to the surface by aluminium tape, and at 15 and 30 mm deep from the exposed panels with 1.5 mm thick sheathed thermocouples. Additional measurements were also made at the exposed side of the unexposed board (45 mm) for the gypsum composite constructions. The location and type of thermocouples used is shown in Figure 5 and Table 3.

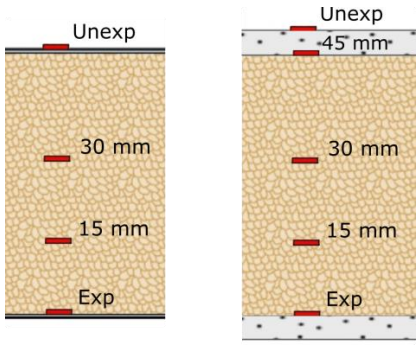

Figure 5: Location of thermocouples

Table 3: Thermocouple type during H-TRIS tests

Thermocouple Positions	Type
Unexposed side-exposed board (Exp in Figure 5)	Copper disk attached with aluminium tape
Cross section	
15 mm	Sheathed thermocouples (1.5 mm)
30 mm	
Exposed side unexposed board (45 mm in Figure 5)	Copper disk attached with aluminium tape
Unexposed side (Unexp in Figure 5)	Copper disk attached with aluminium tape

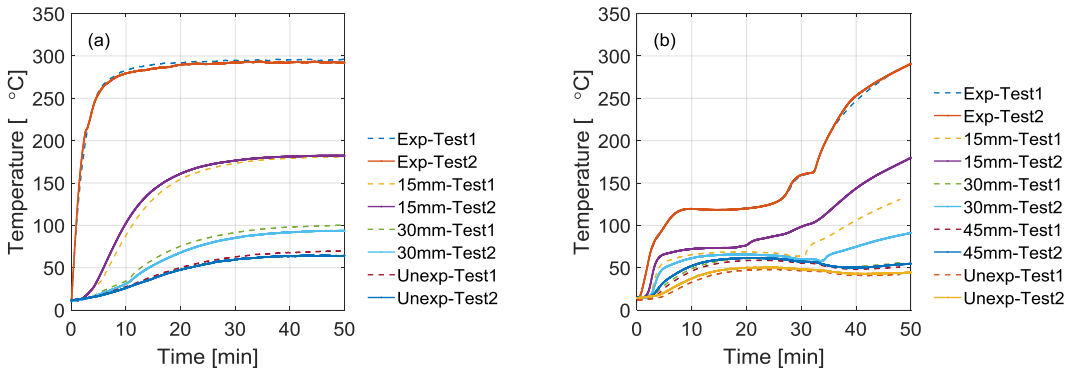

Figure 6: Cross-section temperature measurements for 7 kW/m³ incident radiant heat flux: (a) Test A (S-SW3-S) (b) Test B (G2-SW1-G2)

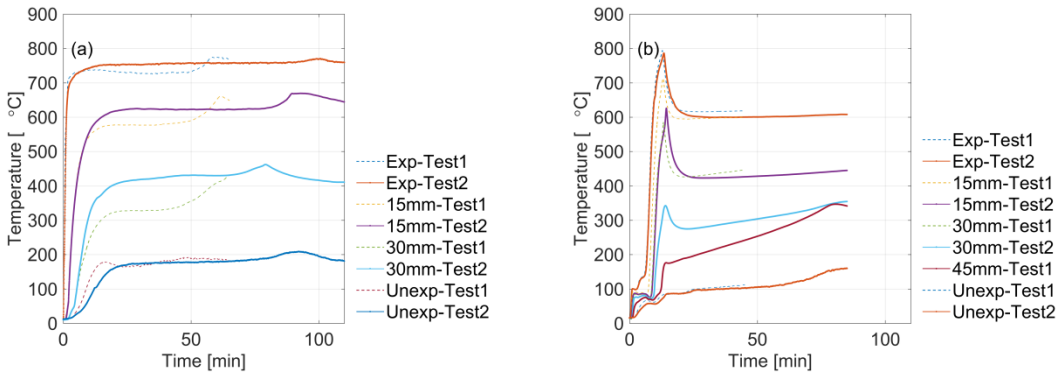

Figure 7: Cross-section temperature measurements for 60 kW/m³ incident radiant heat flux: (a) Test C (S-SW3-S) (b) Test D (G2-SW1-G2)

In general, the tests present good repeatability, especially at low heating rates. The dispersion in temperature readings is lower than 10 % on the unexposed side. Thermocouples showing more dispersed values are the ones located in the stone wool (15 mm and 30 mm), which is likely linked to uncertainty in the exact position of the thermocouple. Figures 6 (a) and 7 (a) show the distribution of temperature for constructions A and B (S-SW3-S), respectively. The exposed panel temperatures show an initial rapid temperature rise followed by a later smooth increase following the heating exposure. There is a slight change in the slope of the temperature curves before 10 minutes, and at 60 kW/m^2, an increase on the temperature is observed after 50-60 minutes into the steady state. Figure 8 shows the binder residue on the exposed side of the unexposed panel and the discolouration of the wool after the test.

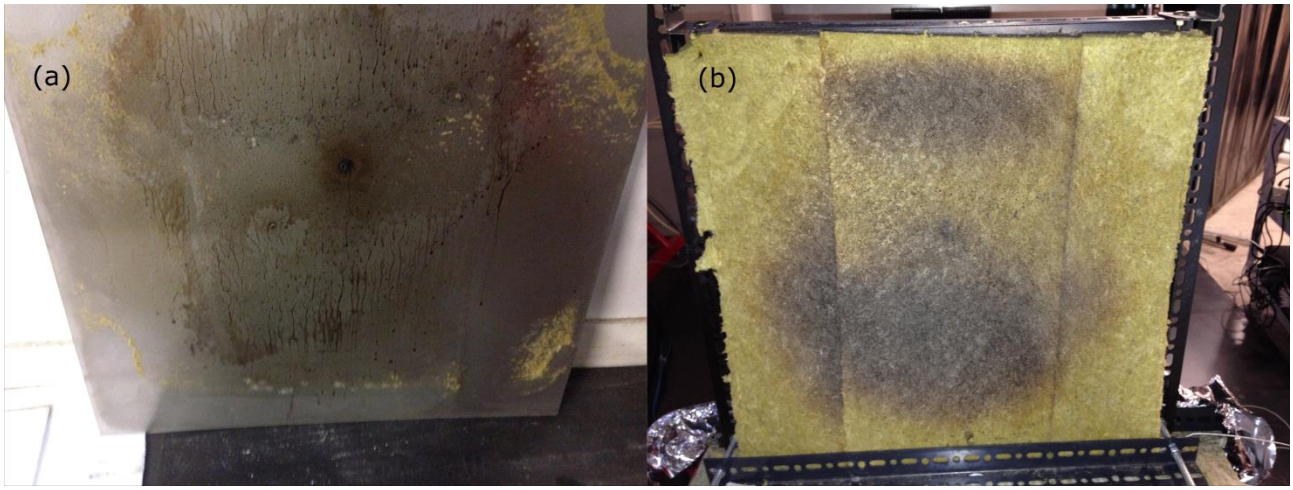

Figure 8: Specimen after test B (60 kW/m²): (a) unexposed steel panel and (b) stone wool.

Figures 6 (b) and 7 (b) show the temperature distribution of the gypsum constructions (tests C and D, respectively) under low and high incident radiant heat fluxes. There is a temperature plateau around 100 °C that corresponds to the evaporation of water from the gypsum plasterboard. The length of the plateau varies with the heating

conditions, being longer for less severe heat exposures. At a low incident radiant heating exposure, in Figure 6 (b), the two-step calcination reaction in the gypsum plasterboard can be observed. At high incident radiant heat flux, in Figure 7(b), after the calcination has taken place there is a rapid increase in temperature. A peak is observed between 10 and 25 minutes, which could be linked to the combustion of the paper lining of the gypsum plasterboard (11). Also, cracking of the board appeared after 10 minutes of exposure, potentially increasing the heat exposure through the cross-section. The thermocouples at 30 mm and 45 mm depths give a steady increase in temperature after the peak, which could be linked to burning of the paper on the unexposed board. Figure 9 (a) shows the unexposed board from the side in contact with the wool (corresponding to 45mm Figure 5) the paper lining burnt around the position of the thermocouple, and Figure 9 (b) the discolouration of the wool after the test.

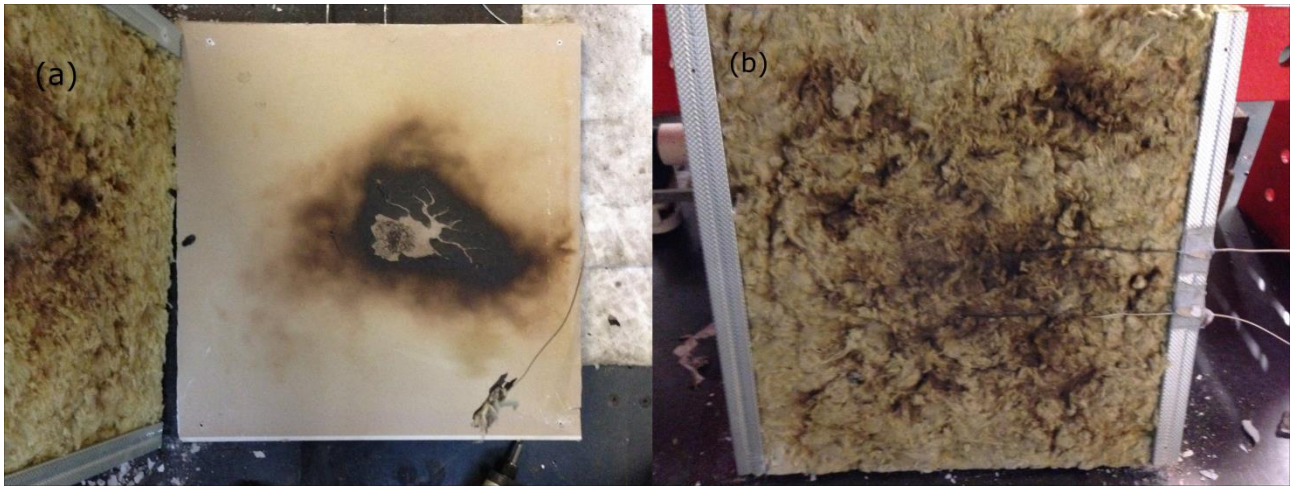

Figure 9: Specimen after Test D (60 kW/m²): (a) unexposed gypsum plasterboard and (b) stone wool.

Variable heat exposures intermediate scale (Phase III)

Parametric like incident heat exposure

Figure 10 shows the temperature measurements for the samples exposed to a parametric-like incident radiant heat exposure in H-TRIS (Tests E-F). The location and type of thermocouples used is the same as in Phase I and II, Table 3 and Figure 5. Figure 10(a) presents the results for Test E (S-SW3-S), showing a smooth increase in temperature following the exposure. As for previous test results, the thermocouples giving more dispersion in the results are the ones located in the wool (15 mm, 30 mm). Around 40 minutes into the test, there is also a bump in temperature values observed along the cross-section. In Test F (G-SW1-G), shown in Figure 10(b), there is also a plateau in the temperatures (at 100°C) due to the dehydration reaction in the gypsum plasterboard, followed by a sudden increase of temperatures and a decay phase. This peak combines the peak previously observed in H-TRIS at constant incident radiant heat fluxes and the peak due to the parametric type exposure.

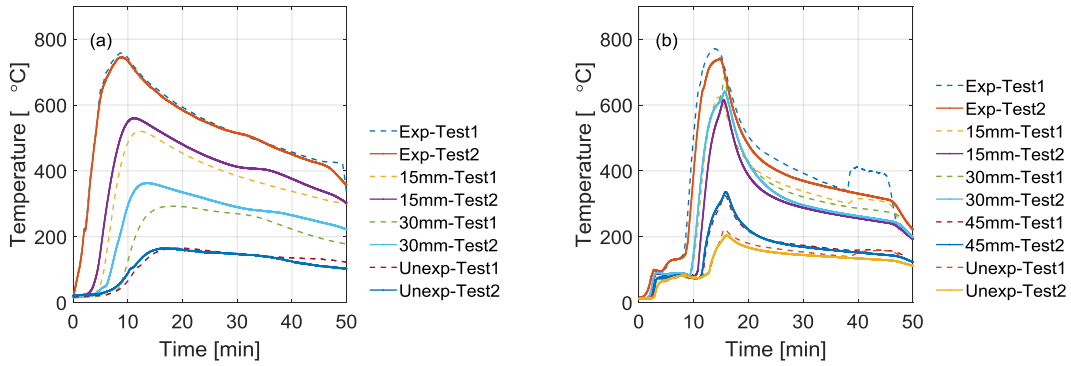

Figure 10: Cross-section temperature measurements for: (a) Test E (S-SW3-S) (b) Test F (G2-SW1-G2)

ISO 834 standard fire curve exposure

Four different constructions were tested under standard ISO 834 exposure in the mid-scale furnace. Figures 11 and 12 show the results for Tests G-H and I-J, respectively. Thermocouples were located similarly as in H-TRIS tests (Figure 5 and Table 3). Temperatures in the cross-section were measured with 1.5 mm thick sheathed thermocouples and on the surface with Type K thermocouples welded to a copper disk and in this case attached to the surface by glued pad, as specified in standard EN 1363-1 (32).

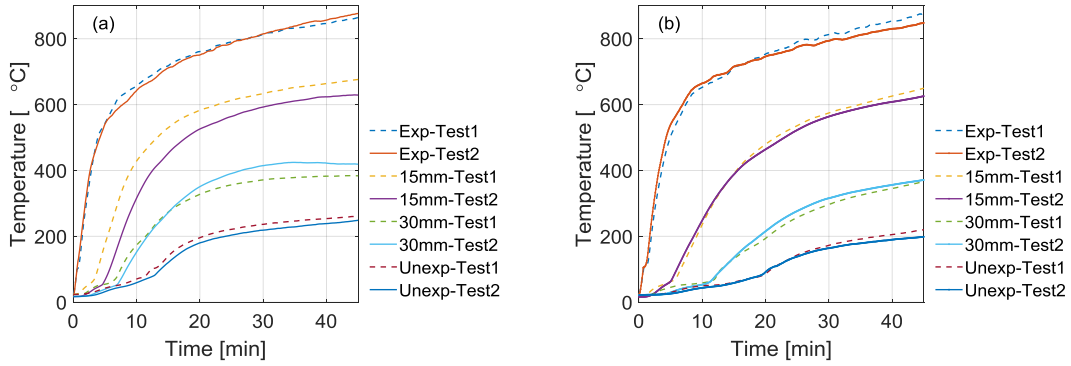

Figure 11: Cross-section temperature measurements for: (a) Test G (S-SW3-S) (b) Test H (S-SW4-S)

The two repeated tests for each of the constructions show good repeatability, with slightly higher uncertainty in thermocouples placed through the cross-section. Temperature profiles are very similar to H-TRIS results with a smooth increase in temperature following the exposure conditions and a change in the slope of the curve between 10-20 minutes. Figure 11(a) and (b) show the difference between different densities of the stone wool, reaching higher temperatures for the wool with lower density. In Figure 12(a-b), the temperature recordings are plotted through the cross-section during Tests I and J, being SW1 (Figure 12a) of lower density than SW2 (Figure 12b). There is more dispersion of the values for the G-SW-G composites compared to the S-SW-S composites. This is due to the more heterogeneous and degradable nature of the gypsum board. The temperature of the exposed board (Exp) is very similar in both cases, meaning

that there is no effect of the density of the wool on the exposed panel behaviour. The length of the temperature plateau is similar in both cases, as are the unexposed side temperatures.

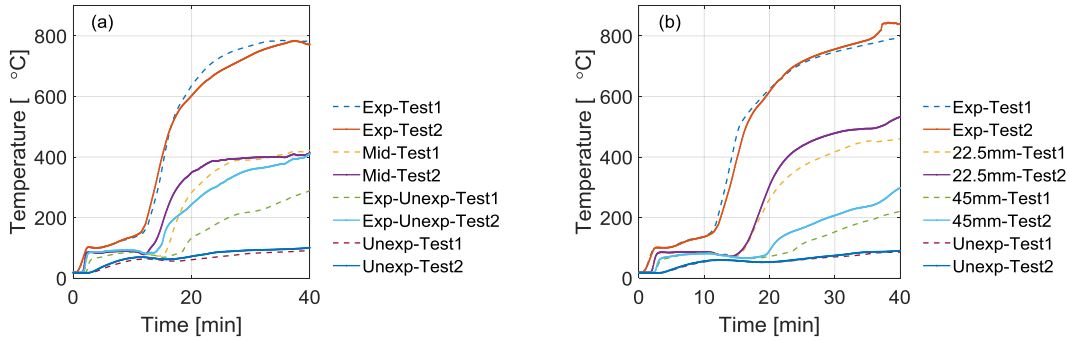

Figure 12: Cross-section temperature measurements for: (a) Test I (G1-SW1-G1) (b) Test J (G1-SW2-G1)

Large-scale ISO 834 furnace test results (Phase IV)

Testing larger dimensions adds complexity to the overall performance of a composite. Thermal bowing and linked stresses, added to singularities in the constructions such as joints, have a considerable influence on the response of the specimens to fire. To investigate this effect and identify which phenomena are present in full-scale testing compared to a smaller scale and other heating conditions, a 3000 x 3000 mm^2 G1-SW2-G1 wall (Test K) was tested under ISO 834 standard time-temperature exposure (1). This corresponds to the same construction that was tested in the mid-scale furnace (Test I) but now includes joints between the 900 x 2500 mm^2 gypsum plasterboards and cold-formed steel studs. According to the addition method, the construction is expected to get an EI-30 rating in a standard ISO 834 furnace test (33,34). Temperatures were recorded at 21 different locations on the unexposed side, using two different attachment methods. Most of the thermocouples were attached following the standard EN 1363-1 (32) method corresponding to thermocouples of Type K welded to a copper disk and attached to the surface by glued pad. Additionally, a few thermocouples were also attached using aluminium tape. Temperature profiles through the cross-sections were measured with 1.5 mm sheathed thermocouples at four different locations in the specimen, and with thermocouples welded onto the steel profiles at two different locations. During Test K, thermal bowing of the wall towards the furnace was observed early during the test. White smoke came out of the upper edges of the wall, probably linked to dehydration of the gypsum plasterboard. At around 13 minutes a crack appeared on the unexposed side of one of the boards, followed by popping out of screws of the adjacent joint. A gap opened increasing subsequently the passage of smoke through this opening. The paper on the unexposed side burned around 35 minutes into the test. The test was stopped at 39 minutes. Figure 13 shows the state of the wall at the end of the test.

Table 4: Thermocouple position during large-scale Test K

Thermocouple Positions	Type	Number of thermocouples
Unexposed side-exposed board (Exp in Figure 5)	Copper disk attached with aluminium tape (A) or glued pad (P)	6
Cross section		
15 mm		6
22.5 mm	Sheathed thermocouples (1.5 mm)	
30 mm		
Exposed side unexposed board (45 mm in Figure 5)	Sheathed thermocouples (1.5 mm)	4
Unexposed side (Unexp in Figure 5)	Copper disk attached with aluminium tape (A) or glued pad (P)	8
Profiles	Welded	9

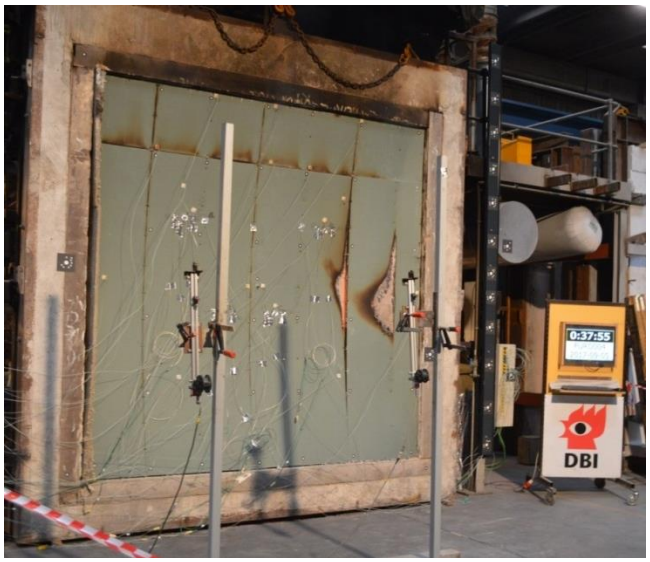

Figure 13: Unexposed side view of the full-scale wall tested at 37 minutes (test K)

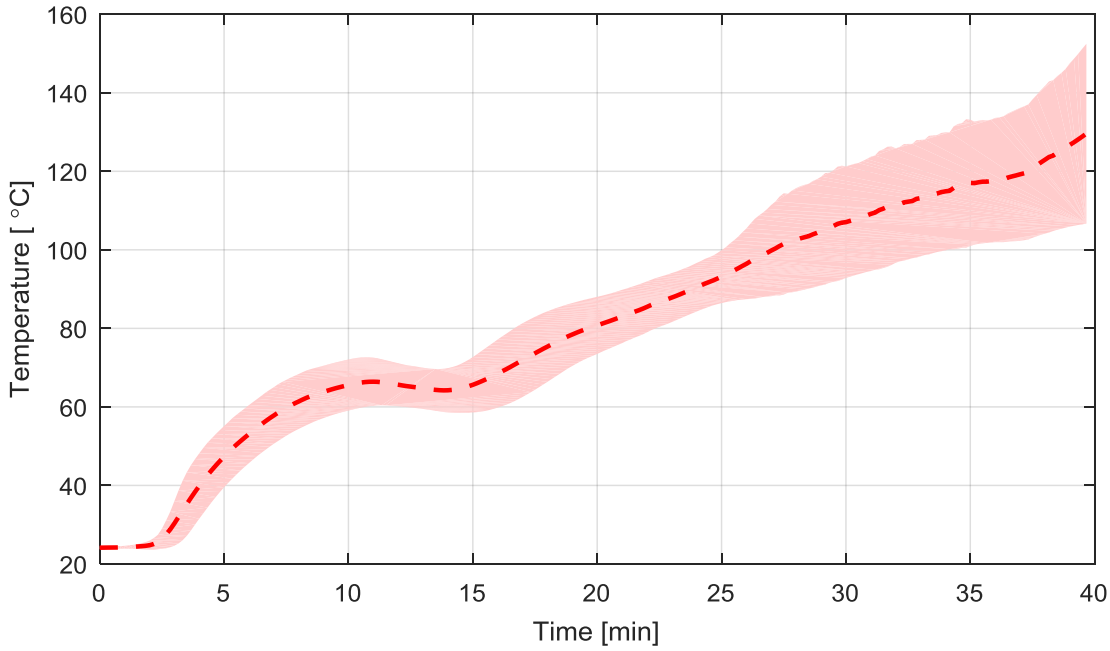

Figure 14: Unexposed side thermocouple readings of G1-SW2-G1 (Large Scale Test K)

Figure 14 plots the mean value (dashed line) and the standard deviation (shade) of all the measurements from thermocouples on the unexposed side of the wall. There is an expected spread on the thermocouple readings on the unexposed side of the panels, linked to the effect of the location in relation to the joint opening and different degradation of the construction induced by mechanical, thermal bowing and cracking on the boards. The cross-section temperature profiles shown in Figure 15 follow similar trends as shown in the mid-scale tests. A temperature plateau is observed around 100 °C and a rapid increase in temperatures afterwards. There is a larger spread on the thermocouple readings through the cross-section once the exposed board is degraded. However, the unexposed side temperature shows a maximum standard deviation of only 14 °C. Figure 16(a) plots the exposed side of the unexposed board measurements; in this case, the thermocouples were not attached to the surface but instead measured with 1.5 mm sheathed thermocouples. Figure 16(b) shows the temperatures measured in the stone wool. The dispersion of these values is linked to (1) the uncertain exact position of the thermocouples, which is difficult to guarantee; (2) temperature measurements in a porous media and flow of hot gases; and (3) cracking and falling-off of the exposed boards.

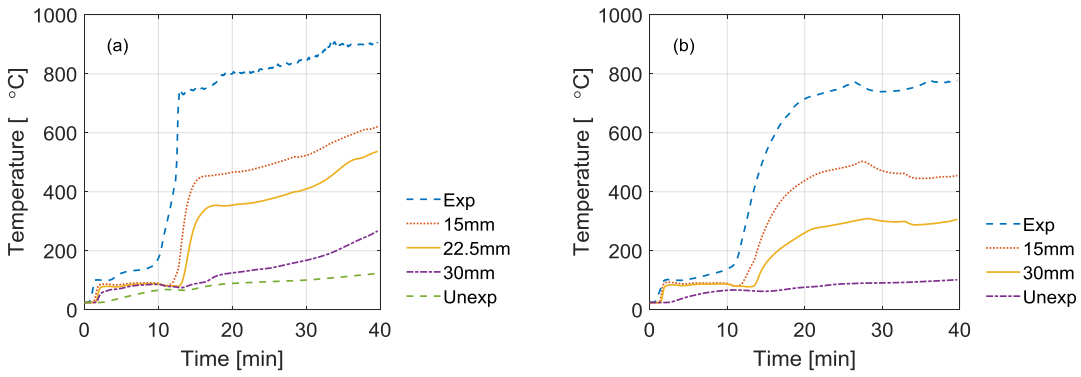

Figure 15: Temperatures through the cross-section in two different locations

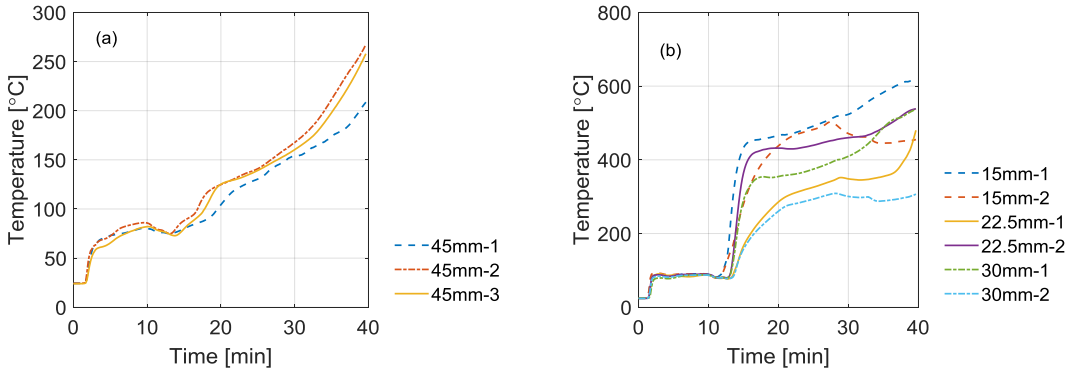

Figure 16: Temperatures exposed side unexposed board and temperatures measured in the wool

Discussion

Testing apparatus

This study presents the experimental results of gypsum-stone wool and steel-stone wool specimens exposed to four different heating exposures, performed in three different testing set-ups (see section 2.3). In addition to the sample sizes, the following considerations need to be taken into account when looking at the results:

- The furnace heats up the volume inside by the combustion of propane-air from the burners. That induces complex heat transfer between the furnace boundaries, the sample, the gas-phase and the burners. Thus, it is more difficult to establish heat transfer coefficients such as view factors or convective heat transfer coefficients than when simply using a radiative panel in an open space, particularly during the early stages of heating which are critical for the types of assemblies and materials considered herein. If temperatures inside the furnace are controlled by plate thermocouples as required in standard ISO 834, adiabatic surface temperatures can be used for modelling instead of convective and radiative boundaries (35).
- Tests in H-TRIS and a large furnace were performed on vertical samples, whereas tests in the mid-scale furnace were performed horizontally. The specimen's orientation affects not only on the exposed and unexposed convective heat transfer

boundaries, but also on how gases move inside the material and on how the heat is transferred through the cross-section and deformation due to gravitational solicitations.

- The oxygen level inside the furnace is about 6 %, which is much lower than in ambient conditions (21 %). The availability of oxygen is a fundamental parameter affecting the way materials combust; therefore different behaviours may be observed in H-TRIS testing as compared to furnace tests. However, which of these conditions is more representative of real fire conditions is not clear as in a fire scenario the oxygen availability depends on ventilation conditions and will vary throughout the duration of the fire.
- In furnace tests, the pressure difference between the inside and the outside will govern pressure driven mass transport through porous media. According to Darcy´s law (Equation 3) the velocity of the mass (ug) is a function of the permeability of the media (κ), the diffusivity (μ_g) and the pressure difference (∇p_g). In tests performed in open conditions (H-TRIS) the pressure difference between the exposed and unexposed side is zero, therefore there is no effect of the pressure differential on the pressure driven mass transport.

$$u_g = -\frac{\kappa}{\mu_g}\nabla p_g \quad [3]$$

Sample size

Sample sizes have a clear effect on the overall performance of samples exposed to fire. However, when looking at one-dimensional heat transfer phenomena and how to accurately model them, performing smaller scale experiments is a powerful tool as it is much faster and more cost-effective. In the current analysis, the same composite (G1-SW1-G1) construction was tested under ISO 834 exposure in the large-scale test (3000 x 3000 mm² Test K in Table 1) and mid-scale (500 x 500 mm² Test I in Table 1). In Test I two repeated tests were performed and Test K had several thermocouples placed at each location (Table 4). Figure 17 plots the test results from the repeated Test I and three thermocouple readings in Test K on the unexposed side of the exposed panel (see Exp in Figure 5) of the sandwich construction and the unexposed side of the specimen (Unexp Figure 5). Figure 17(a) shows reasonable comparable results from the unexposed side temperature measurements between the intermediate scale and the full scale tests. In Figure 17(b), the unexposed side of the exposed panel shows a slightly faster degradation in a larger scale as compared to the intermediate scale. Around 12 minutes in the full scale, two of the thermocouples are providing erroneous readings probably due to cracking-failure of the exposed board. Thus, reduced scale tests can be used as a tool for validating one dimensional thermal models.

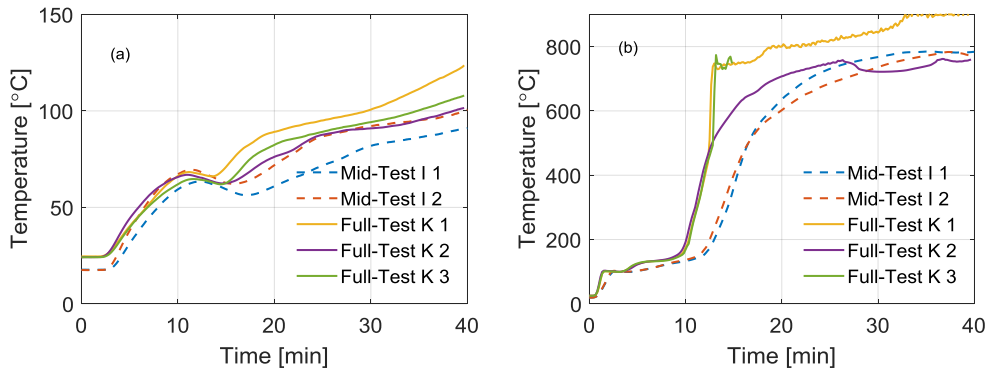

Figure 17: Temperatures from the intermediate furnace test (Test I) and full-scale furnace tests (Test K) (a) Unexposed side of the specimen (Unexp); (b) Unexposed side of the exposed panel (Exp).

Heating exposures

The aim of performing tests under different heat exposures was to identify and isolate the different phenomena that might occur in stone wool layered composites when exposed to severe heating. From micro-scale TGA and MCC test data it was observed that three reactions occur in the wool in an air atmosphere (13,15). If these reactions were occurring in the wool in larger scales (section 1.1), they would be observed in test B (S-SW3-S composite tests at 60 kW/m²). On the contrary, limited reaction would be observed in test A (at 7 kW/m²). In Figure 18 test results of S-SW3-S composites at different heat exposures are plot together. In all temperature plots for S-SW-S composites a change in the slope is observed in early stages of the tests. Additionally, in Figure 7(a), a peak in the temperature is observed through the cross-section of the sample, at around 75 minutes after the test has started; this occurs after 50-60 minutes under steady state. The reaction is detected first by the thermocouple located at 30 mm deep, which is around 400 °C. This peak could be due to the third reaction observed in TGA at 700 °C associated with the crystallisation of the fibres. Tests on steel stone wool composites in the mid-scale furnace showed no peak on the measured temperatures; however, they only lasted for 45 minutes. Figure 19 plots the temperature measurements of the thermocouple placed 30 mm deep in the insulation for three of the different heat exposures, together with the normalised thermal gradients. Three peaks are observed in Figure 19(b) for the 60 kW/m^2 and the ISO 834 exposure before 25 minutes of exposure, whereas only two peaks can be seen at 7 kW/m^2. If no reactions were occurring in the wool, only one peak linked to the heat penetrating the construction would be observed. Thus, the results suggest that certain reactions might be occurring in the wool; however, their effect on temperature increase is smaller than might be expected on the basis of prior testing.

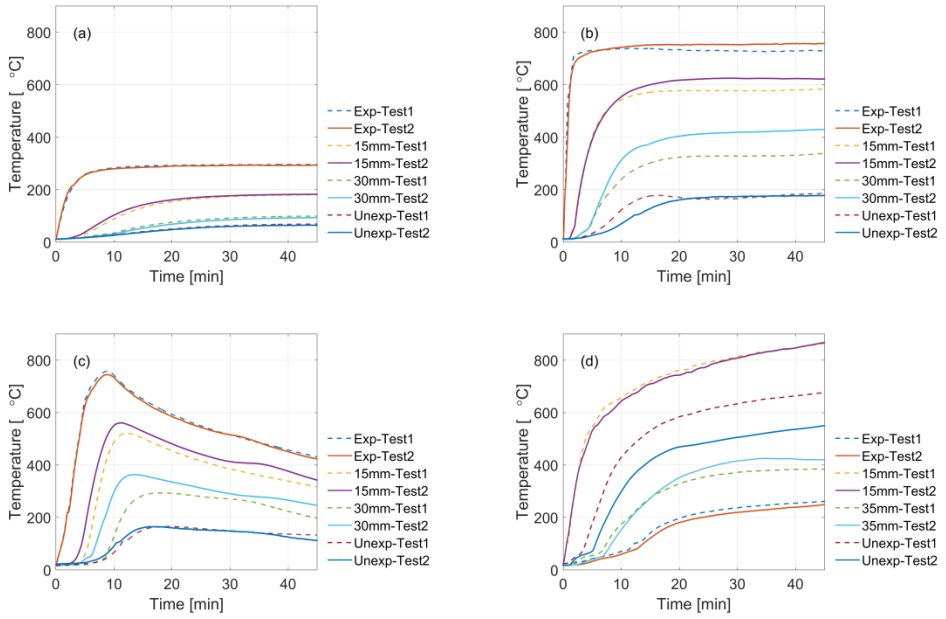

Figure 18: Cross-section temperature measurements for: (a) Test A at 7 kW/m²(S-SW3-S); (b) Test A at 60 kW/m²(S-SW3-S); (c) Test E variable exposure (S-SW3-S); (d) Test G (S-SW3-S) ISO 834

In order to further investigate the effect of wool degradation in composites due to one-sided heat exposure, extra tests were performed on samples with and without a steel shield on the exposed side. The extra tests were performed in a small electric oven where air was supplied constantly, and the temperature time curve provided in ISO 834 was followed as exposures, however the temperatures inside the small oven where controlled with Type K 1.5 mm sheathed thermocouples. In Figure 20 results of the unexposed side surface temperature are plotted for tests performed with a steel-stone wool-steel composite (S-SW-S) and a stone wool-steel composite (SW-S) in the small electric oven. A significant difference is observed between the unexposed temperatures measurements in the two tests performed. The difference could be due to the fact that when there is not a steel plate protecting the exposed side, air is permeating through the wool. These testing conditions are similar to the micro-scale tests where the oxygen required for the reactions to occur is provided. Thus, reactions of organic content and potentially the crystallisation of fibres lead to the peak in temperatures in SW-S, while limited reaction occurred in the wool when a protective layer limited the air entrainment.

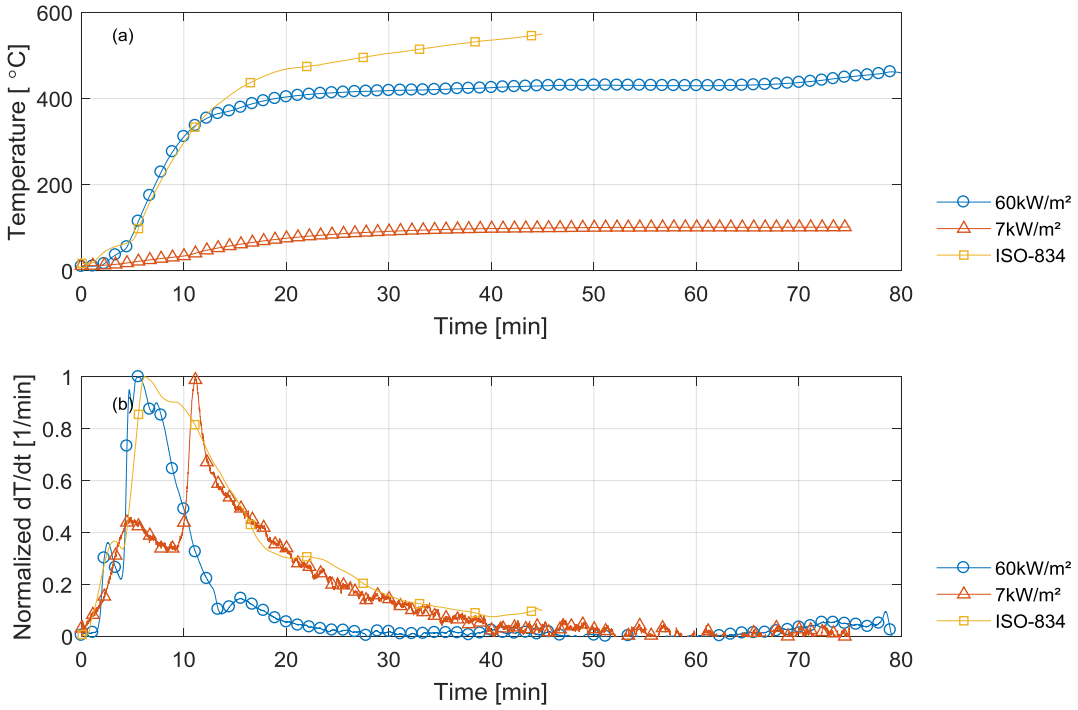

Figure 19: (a) Temperatures measured at 30 mm depth in the S-SW1-S composites; (b) Normalized temperature gradients in time of at 30 mm depth in the S-SW3-S composites.

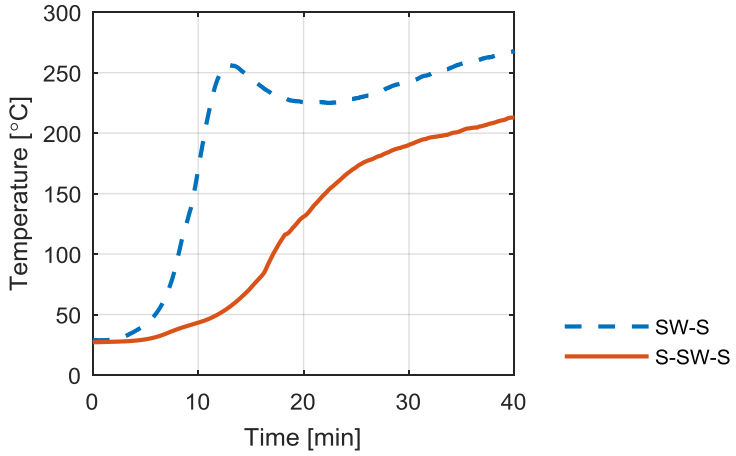

Figure 20: S-SW-S & SW-S composites exposed to the ISO 834 standard fire curve in an electric furnace

In G-SW-G composites (Tests C, D, F, I-K) there are additional effects apart from the wool degradation. For instance, a temperature increase due the two step calcination reaction of the gypsum plasterboard can be observed in Figure 21 (a). The water that is evaporated in this reaction might be travelling through the cross-section of the construction and condensate in colder regions. This would explain the drop in temperature that is observed on the unexposed side of the gypsum composites in all the tests performed. Another potentially important observation from the tests is that after the

temperature plateau in Test D (Figure21(b)), there is a rapid increase in temperature followed by a sharp drop. This peak is also observed in the parametric heat exposure (Test F, Figure 21 (c)); although in this case it is masked by the cooling down effect of the parametric curve. In any case, this is not observed when the samples are tested under ISO 834 standard fire curve (Figures 21(d) and Figure 15-16). This peak could be due to the combustion of the paper layer of the gypsum plasterboard as also observed by Craft et al.(11). This will not occur in furnace tests where the oxygen level could be too low to combust the paper. Due to this phenomenon in the test of G-SW-G composite testing in the H-TRIS, the parametric like incident radiant heat exposure lead to more severe conditions on the unexposed side than ISO 834 fire exposure.

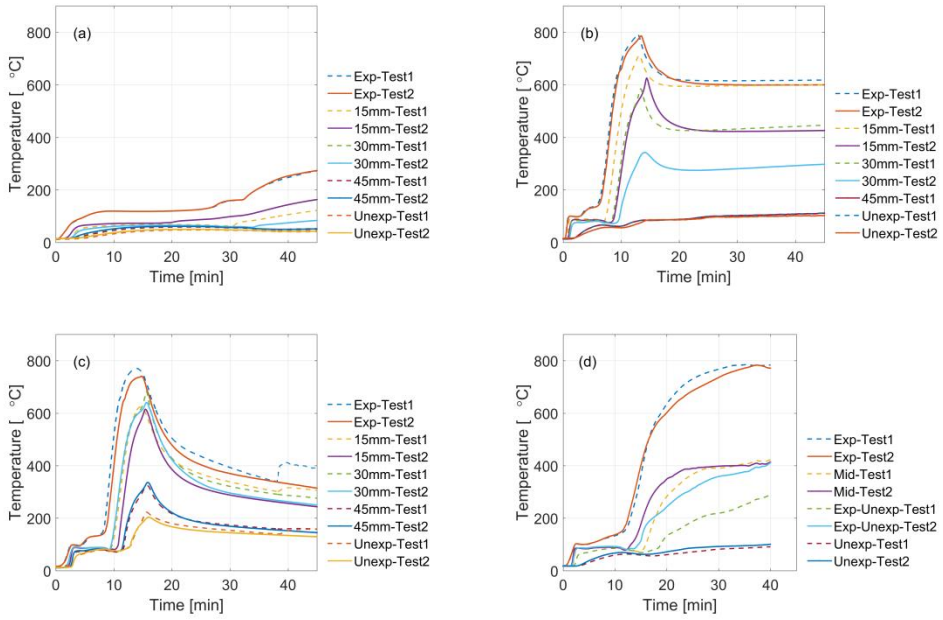

Figure 21: Cross-section temperature measurements for: (a) Test C at 7 kW/m²(G2-SW1-G2); (b) Test D at 60 kW/m²(G2-SW1-G2); (c) Test F variable exposure (G2-SW1-G2); (d) Test I (G1-SW1-G1) ISO 834

Effect of the stone wool

Lower thermal diffusivity (higher density, and lower thermal conductivity) means slower temperature change through the construction. Experimentally, it is difficult to study the effect of changing one material property in isolation as the variation of one or more material properties implies changes in other aspects of the materials, for instance permeability or fibre properties. Numerical studies have shown how a limited variation in stone wool density might have a lesser impact on the unexposed side temperature in standard ISO 834 exposures, compared to variation in the thermal conductivity (36,37). Comparing Test I to Test J for G-SW-G composites (Table 1-2), the stone wool density was 47 % higher and the thermal conductivity was 2 % lower. Furthermore, Test G had a 39 % higher density and 10 % lower ambient thermal conductivity compared to Test H

for S-SW-S composites. The effect of the change on stone wool insulation in a gypsum and steel layered composite is shown in Figure 22. As expected, higher density stone wool and slightly lower ambient thermal conductivity results in a delay on the unexposed side temperatures. The difference is greater in the steel stone wool composites (Figure 22b) because the thermal exposure is higher as there is no delaying effect from the gypsum plasterboard.

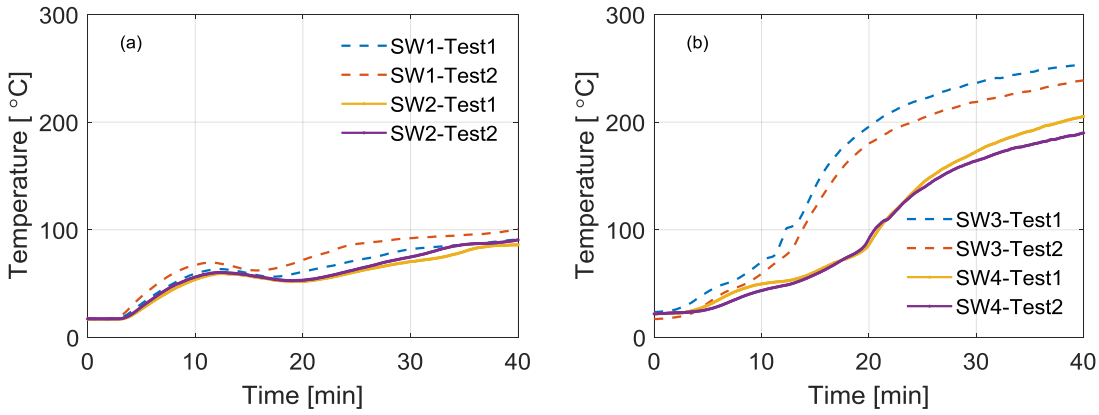

Figure 22: (a) Unexposed side temperature of tests I (G1-SW1-G1) & test J (G1-SW2-G1): (b) Unexposed side temperature of test G (S-SW3-S) & test H (S-SW4-S)

Sensitivity of the analysis to temperature measurements

Test results are strongly dependent on the presence of measurement devices, as they by nature interfere with specimens. In this study, four common approaches to attach thermocouples were followed. In-depth temperatures were measured just by placing sheathed thermocouples at the desired depths. Surface temperatures in the cold-formed steel profiles were measured by welding the thermocouples to the profiles. Unexposed side surface temperatures were measured using two methods of attachment. The first method was to measure unexposed temperature according to EN 1363-1 (32), where a copper disk thermocouple is attached to the unexposed side with a glued pad. The second method was to attach a copper disk thermocouple using aluminium tape. In Figure 23, the temperatures measured on the unexposed side of the panels at four different locations during full-scale Test K are plotted. Measurements performed with thermocouples attached to the surface with aluminium tape gave an average of 11 % higher readings than thermocouples attached with glued pad. Also, temperatures were more susceptible to changes. This difference is because the aluminium tape and the pad have different emissivities, thus affecting the radiative boundary conditions, and because of the glueing effect.

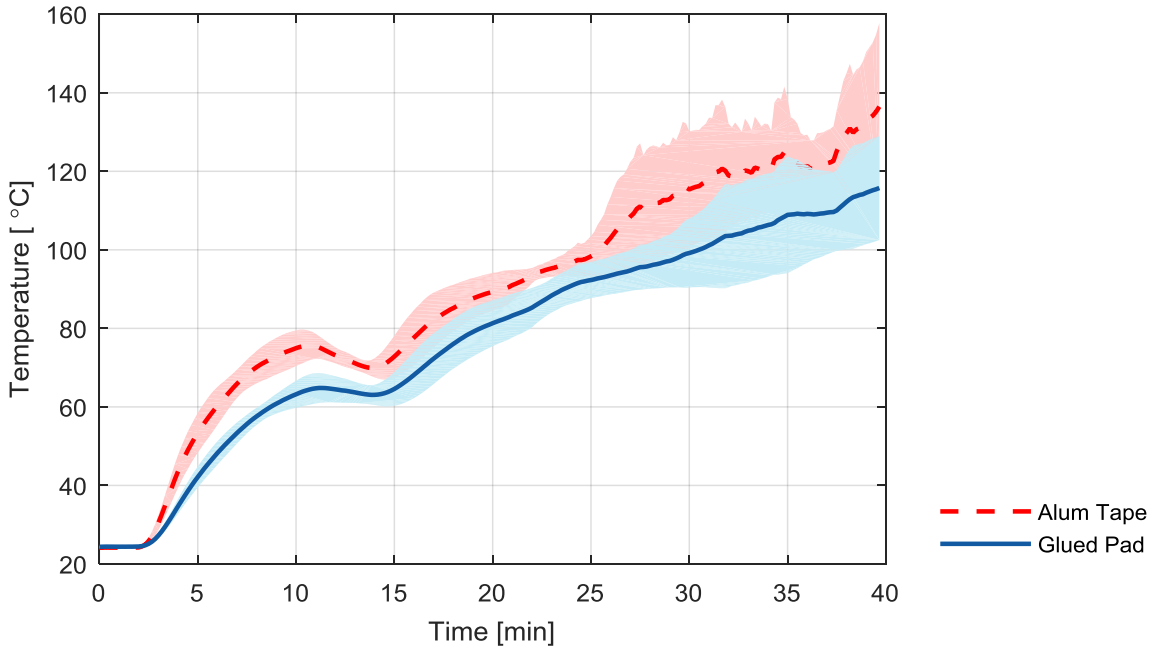

Figure 23: Unexposed side temperatures measurements with thermocouples attached with aluminium tape (A); and glued pad (P) during Test K

Conclusions

Tests on steel-stone wool composites (S-SW-S) and gypsum-stone wool composites (G-SW-G) have been performed under four different heating exposures: (1) 7 kW/m² constant incident radiant heat flux; (2) 60 kW/m² constant incident radiant heat flux; (3) standard ISO 834 time-temperature curve; and (4) parametric-like incident radiant heat exposure. At the lower incident radiant constant heat exposures, samples were maintained in a range of temperatures below 300 °C. In this range of temperatures, limited reaction in the stone wool occurred based on micro-scale TGA and MCC data. Under the other three heat exposures all three expected reactions in the stone wool should occur. However, the effect that the wool reactions have on the temperature profiles appears to be minimal. Thus, the shielding effect of the steel plate on the exposed side, limiting the entrainment of air through the cross-section, appears to limit the oxidative combustion reaction in the organic content and the crystallisation of the fibres. In all of the tests performed on G-SW-G samples, a two-step calcination reaction occurred, followed by a rapid increase in temperature due to degradation of the exposed board, as well as a temperature dip. This drop in temperature could be linked to the water being released from the exposed gypsum that, when it comes in contact with less permeable cold surfaces, condenses and later evaporates. In tests conducted using the H-TRIS method and apparatus at high incident radiant heat exposures, after the calcination occurred a peak in temperatures was observed before reaching steady state. This peak was not observed in furnace tests, and it might be due to the combustion of the paper lining of the gypsum plasterboard not occurring in furnace tests due to low levels of available oxygen.

The oxygen availability is thus a potentially important parameter that might affect the behaviour of layered composites in real fires.

The test results have revealed how different phenomena might occur (or not) in different heating scenarios. Therefore, modelling fire scenarios (e.g. for performance-based design purposes) by using input material properties fitted for a particular fire situation (i.e. standard furnace exposures) might lead to incorrect predictions. The following phenomena identified in this paper ought to be taken into account when developing scenario-independent models:

- The availability of oxygen during tests and how it might affect the burning behaviour, when tests are performed in a furnace or in open conditions as in H-TRIS.
- The organic content reaction in stone wool insulation, which is affected by the air entrainment through the material.
- Two-step dehydration reactions that are typically observed in gypsum plasterboards.
- The drop in temperature in gypsum stone wool layered composites that was observed in the tests presented herein and that might be due to condensation-evaporation cycles.

Testing samples at different scales and under different heating conditions has resulted in a satisfactory understanding of phenomena occurring in stone wool sandwich composites.

Acknowledgments

This study is part of the FIRETOOLS project, which aims to develop prediction methodologies for the fire behaviour of building elements using a scaling approach. The project is collaborative between Lund University and the Danish Institute of Fire and Security Technology. Authors greatly acknowledge FIRETOOLS team, the BRE Centre for Fire Safety Engineering at the University of Edinburgh, and members of the fire lab at the Danish Institute of Fire and Security Technology. Special thanks to Rockwool International A/S.

Funding

This work has been funded by the European Union's Seventh Framework Program under grant no. 316991.

Declaration of Conflict of Interest

The authors declare no conflict of interests

References

1. International Organisation for Standardisation. ISO 834–1:1999: Fire Resistance Tests – Elements of Building Construction – Part 1: General Requirements. 1999;
2. Takeda H. A model to predict fire resistance of non-load bearing wood-stud walls. Fire and Materials. 2003 Jan;27(1):19–39.
3. Keerthan P, Mahendran M. Numerical modelling of non-load-bearing light gauge cold-formed steel frame walls under fire conditions. Journal of Fire Sciences. 2012 Apr 11;30(5):375–403.
4. Craft S, Isgor B, Mehaffey J, Hadjisophocleous G. Modelling Heat And Mass Transfer In Wood-Frame Floor Assemblies Exposed To Fire. Fire Safety Science. 2008;9:1303–14.
5. Takeda H, Mehaffey JR. WALL2D: A model for predicting heat transfer through wood-stud walls exposed to fire. Fire and Materials. 1998 Jul;22(4):133–40.
6. Sultan M, Alfawakhiri F, Benichou N. A model for predicting heat transfer through insulated steel-stud wall assemblies exposed to fire. Fire and Materials, Conference Proceedings. 2001;495–506.
7. Clancy P. Time and probability of failure of timber framed walls in fire. Victoria University of Technology; 1999.
8. Thomas G. Thermal Properties of Gypsum Plasterboard at High Temperatures. Fire and Materials. 2002;26(1):37–45.
9. Keerthan P, Mahendran M. Thermal Performance of Composite Panels Under Fire Conditions Using Numerical Studies: Plasterboards, Rockwool, Glass Fibre and Cellulose Insulations. Fire Technology. 2012;49(2):329–56.
10. Andres B, van Hees P. Experimental and Thermal Analysis of Wall Assemblies Exposed to Standard and Parametric Fires. Proceedings of CONFAB. Glasgow, UK: CONFAB; 2015;
11. Craft ST, Isgor B, Hadjisophocleous G, Mehaffey JR. Predicting the thermal response of gypsum board subjected to a constant heat flux. 2008;333–55.
12. Köning J, Walleij L. Timber frame assemblies exposed to standard and parametric fires. Part 2: A design model for standard fire exposure. 1997.
13. Andres B, Hidalgo JP, Bisby L, Hees P Van. Experimental analysis of stone wool sandwich composites exposed to constant incident heat fluxes and simulated parametric fires. In: Fire and Materials. San Francisco, USA; 2017.

14. Livkiss K, Andres B, Bhargava A, van Hees P. Characterization of stone wool properties for fire safety engineering calculations. Journal of Fire Sciences (under review).
15. Hidalgo JP, Torero JL, Welch S. Experimental Characterisation of the Fire Behaviour of Thermal Insulation Materials for a Performance-Based Design Methodology. Fire Technology. 2016;
16. N N, Didomizio M, Weckman EJ, Roos R. Determination of thermochemical properties of stone wool insulation materials. In: Fire and Materials. San Francisco, USA; 2017.
17. Sjostrom J, Jansson R. Measuring thermal material properties for structural fire engineering. In: 15th International Conference on Experimental Mechanics. 2012.
18. Bentz DP, Flynn DR, Kim JH, Zarr RR. A slug calorimeter for evaluating the thermal performance of fire resistive materials. Fire and Materials. 2006;30(December 2004):257–70.
19. Bentz DP, Gaal PS, Gaal DS. Further Progress in the Development of a Slug Calorimeter for Evaluating the Apparent Thermal Conductivity of Fire Resistive Materials. Proceedings of Thermal Conductivity 29/Thermal Expansion 17. 2008;403–11.
20. Olsen H, Sjöström J, Jansson R, Anderson J. Thermal Properties of Heated Insulation Materials. Proceedings of 13th international Fire and Engineering Conference Interflam. 2013;1049–60.
21. CEN. Eurocode 3: Design of Steel Structures. Part 1-2: General Rules - Structural Fire Design. 2005.
22. Livkiss K, Andres B, Johansson N, Van Hees P. Uncertainties in material thermal modelling of fire resistance tests. In: European symposium of Fire Safety Science. 2015. p. 1–6.
23. Hidalgo JP. Performance-based methodology for the fire safe design of insulation materials in energy efficient buildings. The University of Edinburgh; 2015.
24. Dyrbøl S. Heat transfer in Rockwool modelling and method of measurement. Technical University of Denmark; 1998.
25. EN ISO 1182: Reaction to fire tests for products. Non-combustability test.
26. Sjöström J, Jansson R. Measuring thermal material properties for structural fire engineering. In: 15th International Conference on Experimental Mechanics. Porto; 2012.
27. Park S, Manzello S, Bentz DP, Mizukami T. Determining Thermal Properties of Gypsum Board at Elevated Temperatures. Fire and Materials. 2009;
28. Melinge Y, Lanos C, Nguyen KS, Daiguebonne C, Guillou O, Freslon S. One-Dimensional-Time Study of the Dehydration of Plasterboards Under Standard Fire Condition (ISO 834): Thermo-Chemical Analysis. Journal of Fire Sciences. 2011;29(4):299–316.
29. Maluk C, Bisby L, Krajcovic M, Torero JL. A Heat-Transfer Rate Inducing System (H-TRIS) Test Method. Fire Safety Journal. Elsevier; 2016;
30. Pettersson O, Magnusson SE, Thor J. Fire Engineering Design of Steel Structures. 1976.
31. Incropera FP, DeWitt DP, Bergman TL, Lavine AS. Fundamentals of Heat and Mass Transfer. US Patent 5,328,671. 2007. 997 p.
32. CEN. EN 1363-1:1999 Fire resistance tests-Part 1: General requirements. 2012.
33. EN 1995-1-2:2004 Eurocode 5: Design of Timber Structures, Part1-2: General-Structural Fire Design.
34. Östman B, Mikkola E, Stein R, Frangi A, König J, Dhima D, et al. Fire Safety in Timber Buildings. SP Trätek; 2010.
35. Wickström U. The adiabatic surface temperature and the plate thermometer. In: IAFSS. 2011.
36. Aire CT. Experimental and numerical modeling of heat transfer in wall assemblies. Master Thesis, University of Saskatchewan; 2014.
37. Livkiss K, Andres B, Johansson N, van Hees P. Uncertanties in modelling heat transfer in fire resistance tests: A case study of stone wool sandwich panels. Fire and Materials. 2017;